2008

Hundreds of Milky Way satellites? Luminosity bias in the satellite luminosity function

Erik J. Tollerud

James S. Bullock

Louis E. Strigari

Beth Willman
Haverford College

The Astrophysical Journal, 688:277–289, 2008 November 20

HUNDREDS OF MILKY WAY SATELLITES? LUMINOSITY BIAS IN THE SATELLITE LUMINOSITY FUNCTION

Erik J. Tollerud,[1] James S. Bullock,[1] Louis E. Strigari,[1] and Beth Willman[2]

Received 2008 June 26; accepted 2008 July 25

ABSTRACT

We correct the observed Milky Way satellite luminosity function for luminosity bias using published completeness limits for the Sloan Digital Sky Survey DR5. Assuming that the spatial distribution of Milky Way satellites tracks the subhalos found in the Via Lactea ΛCDM *N*-body simulation, we show that there should be between ∼300 and ∼600 satellites within 400 kpc of the Sun that are brighter than the faintest known dwarf galaxies and that there may be as many as ∼1000, depending on assumptions. By taking into account completeness limits, we show that the radial distribution of known Milky Way dwarfs is consistent with our assumption that the full satellite population tracks that of subhalos. These results alleviate the primary worries associated with the so-called missing satellites problem in CDM. We show that future, deep wide-field surveys such as SkyMapper, the Dark Energy Survey (DES), PanSTARRS, and the Large Synoptic Survey Telescope (LSST) will deliver a complete census of ultrafaint dwarf satellites out to the Milky Way virial radius, offer new limits on the free-streaming scale of dark matter, and provide unprecedented constraints on the low-luminosity threshold of galaxy formation.

Subject headings: cosmology: observations — galaxies: dwarf — galaxies: halos — Local Group — surveys

Online material: color figures

1. INTRODUCTION

It is well established from simulations in the ΛCDM concordance cosmology that galaxy halos are formed by the merging of smaller halos (e.g., Stewart et al. 2008 and references therein). As a result of their high formation redshifts and correspondingly high densities, a large number of self-bound dark matter subhalos should survive the merging process and exist within the dark matter halos of L_* galaxies like the Milky Way (Klypin et al. 1999; Moore et al. 1999; Zentner & Bullock 2003). A direct confirmation of this prediction has yet to occur. Surveys of the halos of the Milky Way (e.g., Willman et al. 2005; Belokurov et al. 2006; Walsh et al. 2007; Belokurov et al. 2008) and Andromeda (e.g., Martin et al. 2006; Majewski et al. 2007; Irwin et al. 2008; McConnachie et al. 2008) have revealed only ∼20 luminous dwarf satellites around each galaxy, approximately 1 order of magnitude fewer than the expected number of subhalos that are thought to be massive enough to form stars (Klypin et al. 1999; Moore et al. 1999; Diemand et al. 2007b; Strigari et al. 2007b). Of course, the mismatch is much more extreme (larger than a factor of $\sim 10^{10}$) when compared to the full mass function of CDM subhalos, which is expected to rise as $\sim 1/M$ down to the small-scale clustering cutoff for the dark matter particle, $M_{\rm cut} \ll 1\ M_\odot$ (Hofmann et al. 2001; Bertschinger 2006; Profumo et al. 2006; Johnson & Kamionkowski 2008).

Astrophysical solutions to this missing satellites problem (MSP) include a reduction in the ability of small halos to accrete gas after reionization (Bullock et al. 2000; Somerville 2002; Benson et al. 2002) and tidal stripping, which shrinks the mass of halos *after* they have formed stars (Kravtsov et al. 2004). Although there are some promising new techniques in development for studying the formation of low-mass galaxies within a CDM context (Robertson & Kravtsov 2008; Kaufmann et al. 2007; Orban et al. 2008), current models have trouble explaining many details, particularly regarding the lowest luminosity dwarfs (see below). Other more exotic solutions rely on dark matter particles that are not cold (Hogan & Dalcanton 2000; Kaplinghat 2005; Cembranos et al. 2005; Strigari et al. 2007c) or nonstandard models of inflation (Zentner & Bullock 2003), which produce small-scale power spectrum cutoffs at $M_{\rm cut} \sim 10^6$–$10^8\ M_\odot$, well above the cutoff scale in standard ΛCDM. In principle, each of these scenarios leaves its mark on the properties of satellite galaxies, although multiple scenarios fit the current data. Hence, precisely determining the shape and normalization of the lowest end of the luminosity function is critical to understanding how faint galaxies form and how the efficiency of star formation is suppressed in the smallest dark matter halos.

The Sloan Digital Sky Survey (SDSS; Adelman-McCarthy et al. 2007) has revolutionized our view of the Milky Way and its environment, doubling the number of known dwarf spheroidal (dSph) galaxies over the last several years (e.g., Willman et al. 2005; Zucker et al. 2006a, 2006b; Belokurov et al. 2006; Grillmair 2006; Walsh et al. 2007; Irwin et al. 2007). Many of these new dSph galaxies are ultrafaint, with luminosities as low as $\sim 1000\ L_\odot$, faint enough to evade detection in surveys with limits sufficient for detecting most previously known Local Group dwarfs (Whiting et al. 2007). In addition to providing fainter detections, the homogeneous form of the SDSS allows for a much better understanding of the statistics of detection. Unfortunately, given the inherent faintness of the newly discovered dSph's and the magnitude-limited nature of SDSS for such objects, a derivation of the full luminosity function of satellites within the Milky Way halo must include a substantial correction for more distant undetectable satellites. Koposov et al. (2008) provided an important step in this process by performing simulations in order to quantify the detection limits of the SDSS and estimated the luminosity function by applying these limits to some simple radial distribution functions, finding ∼70 satellites and a satellite luminosity function consistent with a single power law of the form $dN/dL_V \sim L^{-1.25}$.

[1] Center for Cosmology, Department of Physics and Astronomy, University of California at Irvine, Irvine, CA 92697.

[2] Harvard-Smithsonian Center for Astrophysics, 60 Garden Street, Cambridge, MA 02138.

Our aim is to take the detection limits for SDSS Data Release 5 (DR5) as determined by Koposov et al. (2008) and combine them with a CDM-motivated satellite distribution. In order to provide a theoretically motivated estimate for the total number of Milky Way satellite galaxies, we adopt the distributions of subhalos in the Via Lactea simulation (Diemand et al. 2007a) and assume these to be hosts of satellite galaxies. Note that for the purposes of this paper, we define a galaxy as a stellar system that is embedded in a dark matter halo.

The organization of this paper is as follows: In § 2 we describe the overall strategy and sources of data used for this correction, as well as discussing the validity of the assumptions underlying these data. Section 3 describes in detail how the correction is performed and presents the resulting luminosity functions for a number of possible scenarios, while § 4 discusses the prospects for detecting the as yet unseen satellites that the correction predicts. Section 5 discusses some of the caveats associated with the technique used for this correction, as well as the cosmological implications of the presence of this many satellite galaxies. In § 6 we draw some final conclusions.

2. APPROACH AND DATA SOURCES

2.1. *Strategy*

The luminosity bias within the SDSS survey can be approximated by a characteristic heliocentric completeness radius, $R_{\rm comp}(M_V)$, beyond which a dwarf galaxy of absolute magnitude M_V cannot be observed. This radial incompleteness is accompanied by a more obvious angular incompleteness; the SDSS DR5 covers only a fraction $f_{\rm DR5} = 0.194$ of the sky, or a solid angle $\Omega_{\rm DR5} = 8000$ deg^2. For the corrections presented in § 3, we assume that magnitude M_V satellites with heliocentric distances $r > R_{\rm comp}(M_V)$ have not been observed, while satellites with $r \leq R_{\rm comp}(M_V)$ have been observed, provided that they are situated within the area of the sky covered by the SDSS footprint. Given an observed number of satellites brighter than M_V within the survey area $\Omega_{\rm DR5}$ and within a radius $r = R_{\rm comp}(M_V)$, we aim to determine a correction factor, c, that gives the total number of satellites brighter than M_V within a spherical volume associated with the larger outer radius $R_{\rm outer}$, $N_{\rm tot} = c(r, \Omega)N_{\rm obs}(< r, < \Omega)$. For our main results, we count galaxies within $R_{\rm outer} = 417$ kpc, corresponding to the distance to the outermost Milky Way satellite (Leo T), although we do consider other $R_{\rm outer}$ values in § 3.

It is useful (although not precisely correct) to think of the correction factor as a multiplicative combination of a radial correction factor and an angular correction factor, $c = c_r c_\Omega$. The first correction, c_r, will depend on the radial distribution of satellites. If there is no systematic angular bias in the satellite distribution and if the experiment is performed many times, then the second correction factor should have an average value $\langle c_\Omega \rangle = 1/f_{\rm DR5} = 5.15$. However, if the satellite distribution is anisotropic on the sky, the value of c_Ω for any particular survey pointing may be significantly different from the average. An estimate of this anisotropy is essential in any attempt to provide a correction with meaningful errors. Below, we use the satellite halo distribution in Via Lactea to provide an estimate for the overall correction (see § 2.3). Note that in our final corrections presented in § 3, we do not force the radial and angular corrections to be separable, but rather use a series of mock survey pointings within the simulation to calculate an effective correction, $c = c(r, \Omega)$, satellite by satellite.

2.2. *SDSS Detection Limits*

Koposov et al. (2008) constructed an automated pipeline to extract the locations of Milky Way satellites from the DR5 stellar catalog. They then constructed artificial dSph galaxy stellar populations (assuming a Plummer distribution), added them to the catalog, and ran their pipeline. The detections of galaxies were used to construct detection thresholds as a function of distance (Koposov et al. 2008, their Fig. 8). These thresholds are mostly constant as a function of surface brightness for $\mu \lesssim 30$ and linear with the logarithm of distance. Hence, their detection threshold is well approximated as a log-linear relationship between the absolute magnitude of a dSph galaxy, M_V, and the volume, $V_{\rm comp}(M_V)$, out to which the DR5 could detect it. Specifically, Figure 13 of Koposov et al. (2008) implies

$$V_{\rm comp} = 10^{(-aM_V - b)}\ {\rm Mpc}^{-3}, \qquad (1)$$

such that the completeness volume follows $V_{\rm comp} \propto L_V^{5a/2}$. We adopt this form as the dwarf galaxy detection limit of DR5. This volume may be related to a spherical completeness radius, $R_{\rm comp}$, beyond which a dSph of a particular magnitude will go undetected:

$$R_{\rm comp}(M_V) = \left(\frac{3}{4\pi f_{\rm DR5}}\right)^{1/3} 10^{(-aM_V - b)/3}\ {\rm Mpc}, \qquad (2)$$

where $f_{\rm DR5} = 0.194$ is the fraction of the sky covered by DR5. For our fiducial relation, we use the result presented in Koposov et al. (2008, their Fig. 13), which is fit by $a = 0.60$ and $b = 5.23$. We note that for this value of a, we have $R_{\rm comp} \approx 66\ {\rm kpc}(L/1000\ L_\odot)^{1/2}$, and the SDSS is complete down to a fixed *apparent* luminosity. The implied relationship between galaxy luminosity and corresponding heliocentric completeness radius is shown by the solid curve in Figure 1. We also consider

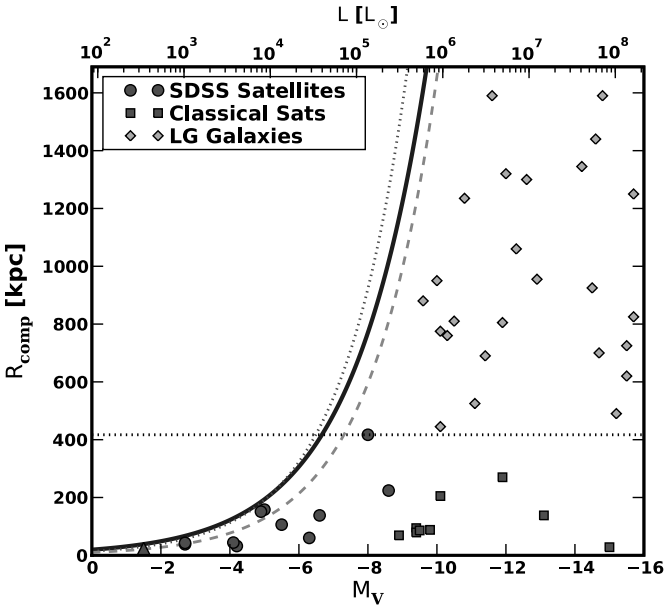

FIG. 1.—Completeness radius for dwarf satellites. The three rising curves show the heliocentric distance, $R_{\rm comp}$, out to which dwarf satellites of a given absolute magnitude are complete within the SDSS DR5 survey. The solid curve is for the published detection limits in Koposov et al. (2008), and the other curves are for the other two detection limits described in § 2.2. The dotted horizontal black line at 417 kpc corresponds to our fiducial adopted outer edge of the Milky Way halo satellite population ($R_{\rm outer}$). The data points are observed satellites of the Milky Way and the Local Group. The circles are the SDSS-detected satellites, the only galaxies to which the detection limits actually apply, although the detection limits nevertheless also delineate the detection zone for more distant Local Group galaxies (*diamonds*). Squares indicate classical Milky Way satellites. The faintest object (*triangle*) is Segue 1, which is outside the DR5 footprint. [*See the electronic edition of the Journal for a color version of this figure.*]

TABLE 1
PROPERTIES OF KNOWN MILKY WAY SATELLITE GALAXIES

Satellite	M_V	L_V ($L_\odot$)	$d_{\rm Sun}$ (kpc)	$R_{\rm half}$ (kpc)[a]	ϵ[b]
SDSS-discovered Satellites					
Boötes I[c]	−6.3	2.83×10^4	60	242	1.0
Boötes II[c]	−2.7	1.03×10^3	43	72	0.2
Canes Venatici I[c]	−8.6	2.36×10^5	224	565	0.99
Canes Venatici II[c]	−4.9	7.80×10^3	151	74	0.47
Coma[c]	−4.1	3.73×10^3	44	77	0.97
Hercules[c]	−6.6	3.73×10^4	138	330	0.72
Leo IV[c]	−5.0	8.55×10^3	158	116	0.79
Leo T	−8.0	5.92×10^4	417	170	0.76
Segue 1[d]	−1.5	3.40×10^2	23	29	1.0
Ursa Major I[c]	−5.5	1.36×10^4	106	318	0.56
Ursa Major II[c]	−4.2	4.09×10^3	32	140	0.78
Willman 1[c]	−2.7	1.03×10^3	38	25	0.99
Classical (pre-SDSS) Satellites					
Carina	−9.4	4.92×10^5	94	210	...
Draco[c]	−9.4	4.92×10^5	79	180	1.0
Fornax	−13.1	1.49×10^7	138	460	...
LMC	−18.5	2.15×10^9	49	2591	...
Leo I	−11.9	4.92×10^6	270	215	1.0
Leo II[c]	−10.1	9.38×10^5	205	160	1.0
Ursa Minor	−8.9	1.49×10^5	69	200	...
SMC	−17.1	5.92×10^8	63	1088	...
Sculptor	−9.8	7.11×10^5	88	110	...
Sextans	−9.5	5.40×10^5	86	335	...
Sagittarius	−15	8.55×10^7	28	125	...

NOTE.—Data are from Bothun & Thompson (1988), Mateo (1998), Grebel et al. (2003), Simon & Geha (2007), Martin et al. (2008), and de Jong et al. (2008).
[a] Satellite projected half-light radius.
[b] Detection efficiency from Koposov et al. (2008).
[c] Galaxy is situated within the SDSS DR5 footprint.
[d] Satellite is not used in fiducial LF correction.

two alternative possibilities. One is obtained by fitting the data in Koposov et al. (2008, their Table 3), which gives $a = 0.684$ and $b = 5.667$ (*dotted curve*), and the other is a line that passes through the new SDSS satellites, on the assumption that some of them are of marginal detectability ($a = 0.666$ and $b = 6.10$; *dashed curve*).

It is important to recognize that, in principle, the detectability of satellites at a particular radius is not a step function between detection and nondetection. It also should not be spherically symmetric (independent of latitude with respect to the disk plane), nor should it be independent of other variables (such as satellite color or background galaxy density). However, Koposov et al. (2008) found that a simple radial dependence provided a good description of their simulation results, and we adopt it for our corrections here. They did, however, find that galaxies within this "completeness" boundary were not always detected at 100% efficiency (depending on their distance and luminosity) and published detection efficiencies for the known SDSS dwarfs (their Table 3). We use these published detection efficiencies in our fiducial corrections to the luminosity function below. We also investigate how our results change when we assume 100% efficiency in the correction.

For reference, the horizontal dotted line in Figure 1 marks our fiducial adopted $R_{\rm outer}$ radius for the Milky Way halo (slightly larger than the virial radius, in order to include Leo T). According to this estimate, only satellites brighter than $M_V \simeq -7$ are observable out to this radius. The fact that the faintest dwarf satellite galaxies known are more than 4 mag fainter than this limit (see Table 1) immediately suggests that there are many more faint satellite galaxies yet to be discovered.

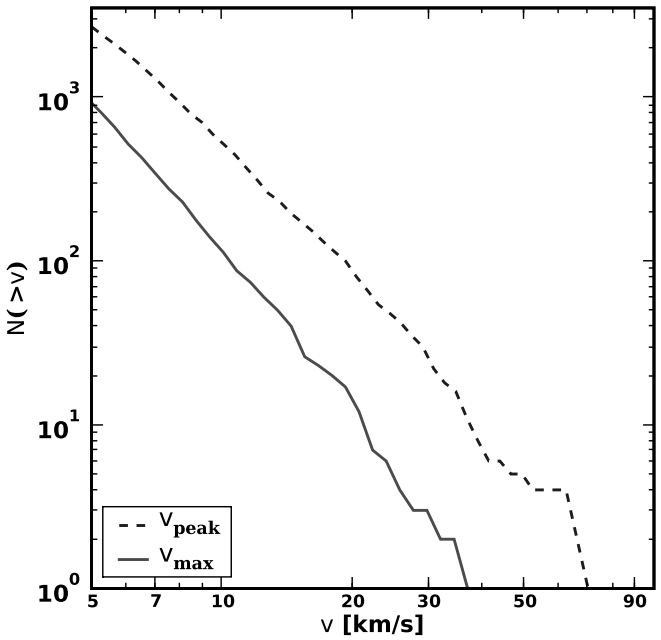

FIG. 2.—Cumulative count of Via Lactea subhalos as a function of the (current) maximum circular velocity of the subhalo ($v_{\rm max}$; *solid line*) and as a function of the largest maximum circular velocity ever obtained by the subhalo ($v_{\rm peak}$; *dashed line*). [*See the electronic edition of the Journal for a color version of this figure.*]

2.3. *Via Lactea*

Diemand et al. (2007a) describe the Via Lactea simulation, which is among the highest resolution ΛCDM N-body simulations of a Milky Way–like dark matter halo yet published. The mass of Via Lactea is $M_{200} \simeq 1.8 \times 10^{12}\ M_\odot$, with a corresponding virial radius $R_{200} = 389$ kpc, where M_{200} and R_{200} are defined by the volume that contains 200 times the mean matter density. It resolves a large amount of substructure, recording 6553 subhalos with peak circular velocities larger than 5 km s^{-1} at some point in their history, of which 2686 are within our adopted $R_{\rm outer} = 417$ kpc at $z = 0$. We use the public data release kindly provided by Diemand et al. (2007a) in what follows.[3]

Figure 2 presents the cumulative maximum circular velocity function, $N(> v_{\rm max})$, for Via Lactea subhalos with halocentric radius $R < 417$ kpc at $z = 0$ (*solid line*), along with the cumulative "peak" circular velocity function (*dashed line*) for the same halos $N(> v_{\rm peak})$. Here $v_{\rm peak}$ is the maximum circular velocity that the subhalos *ever* had over their history. As emphasized by Kravtsov et al. (2004), many subhalos have lost considerable mass over their history, and therefore $v_{\rm peak}$ may be a more reasonable variable to associate with satellite visibility than the (current) subhalo $v_{\rm max}$. The information contained within this figure is presented elsewhere in the literature (Diemand et al. 2007a), although we include it here for the sake of completeness.

An important ingredient in the luminosity bias correction is the assumed underlying radial distribution of satellites. We determine this distribution directly from Via Lactea. We are interested in determining the total number of satellites, $N_{\rm tot}$, given an observed number within a radius, $N_{\rm obs}(<r)$. The correction will depend on the cumulative fraction of objects within a radius r compared to the total count within some fiducial outer radius,

[3] See http://www.ucolick.org/~diemand/vl/data.html.

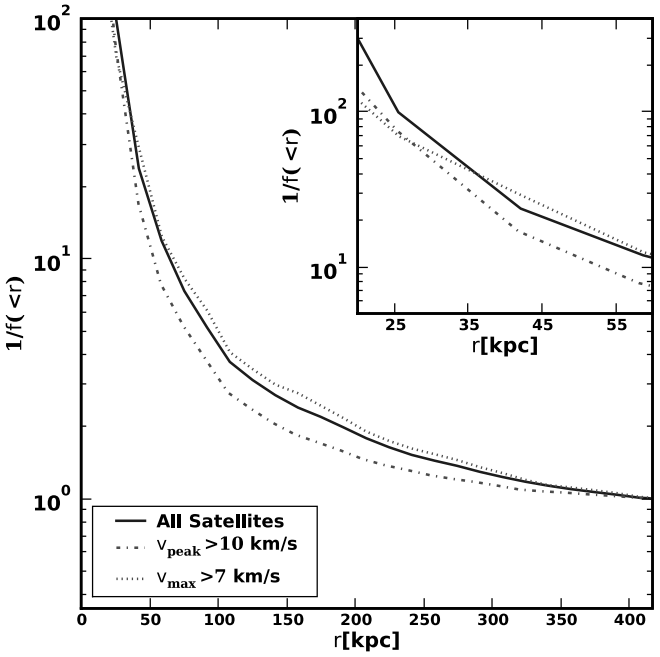

FIG. 3.—Inverse of cumulative subhalo counts within the specified radius. Here $f(<r)$ is the fraction of subhalos that exist within a given radius, normalized to unity at $R_{\rm outer} = 417$ kpc. The radius is "heliocentric," defined relative to the (8, 0, 0) kpc position of the Via Lactea simulation. We include three populations of subhalos, as identified in the key. The inset focuses on the radial range, where most of the new ultrafaint SDSS satellites have been detected. [*See the electronic edition of the Journal for a color version of this figure.*]

$f(<r) = N(<r)/N_{\rm tot}$. The associated radial correction factor is then the inverse of the cumulative fraction, $c_r = f^{-1}(<r)$, such that $N_{\rm tot} = c_r N_{\rm obs}(<r)$. This correction factor is shown in Figure 3 for three different choices of subhalo populations: $v_{\rm peak} > 10$ km s^{-1}, $v_{\rm max} > 7$ km s^{-1}, and $v_{\rm peak} > 5$ km s^{-1} (i.e., all subhalos in the Via Lactea catalog).

In order to mimic a heliocentric radial distribution, in Figure 3 we have placed the observer at a radius of 8 kpc within a fictional disk centered on Via Lactea. The orientation of the "disk" was chosen to be in the Via Lactea xy-plane for all figures that show subhalo distributions, but we allow for a range of disk orientations for the full correction presented in § 3. We do this for completeness, but stress that our results are extremely insensitive to the choice of solar location and are virtually identical if we simply adopt a vantage point from the center of Via Lactea. The total count is defined within our fiducial $R_{\rm outer}$, such that $f(<417\ {\rm kpc}) = 1.0$. An important result of this is that our correction does not depend on the number of subhalos in Via Lactea, only on the shape of the distribution. Still, the shape varies among some subpopulations of subhalo. As noted in Kravtsov et al. (2004), Diemand et al. (2007a), and Madau et al. (2008), subhalos chosen to have a large $v_{\rm peak}$ tend to be more centrally concentrated. However, the correction we apply is fairly insensitive to the differences between these choices of subhalo populations.

The most important corrections will be those for the faintest galaxies, which are just observable at local distances $r \lesssim 50$ kpc. It is thus clear that the radial correction factors associated with the three different subhalo populations show very little differences at the radii of relevance (see Fig. 3, *inset*). Motivated by this result, we use the full Via Lactea subhalo catalog in our fiducial model, because it provides a larger statistical sample of subhalos. However, for the sake of completeness, we present the final corrected

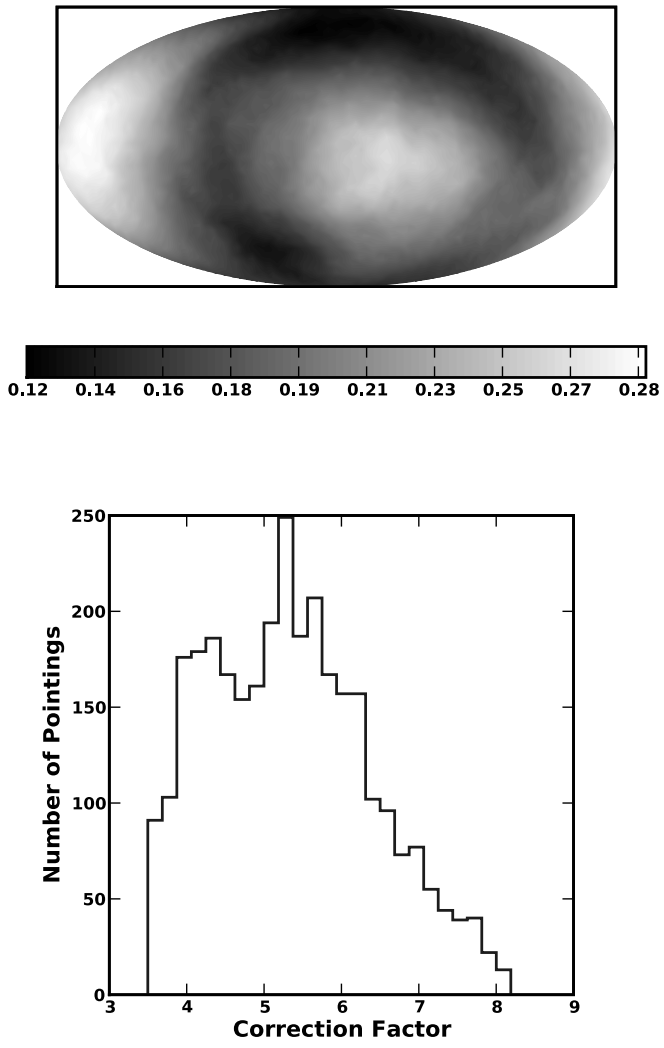

FIG. 4.—Example of subhalo angular anisotropy. *Top*: Hammer projection map of the angular anisotropy in Via Lactea subhalos with $v_{\rm peak} > 5$ km s^{-1}. Colors at each point indicate the fraction of subhalos, $f(<\Omega)$, within 417 kpc that are contained within an angular cone of $\Omega_{\rm DR5} = 8000$ deg^2, in order to match the area of SDSS DR5. *Bottom*: Distribution of the angular correction factors, $c_\Omega = 1/f(<\Omega)$, which must be applied to the count within 8000 deg^2 in order to return the full number of subhalos within 417 kpc. The histogram includes 1000 pointings, evenly spaced over the sky. For reference, the sky coverage of DR5 is $f_{\rm DR5} = 0.194$, which implies an angular correction factor of $1/f_{\rm DR5} = 5.15$. As it must, $c = 5.15$ matches the mean of the distribution, but not the median, which is $c = 5.27$. Note that these correction factors do not yet include the effects of radial incompleteness/luminosity bias. [*See the electronic edition of the Journal for a color version of this figure.*]

counts for our corrections using the $v_{\rm peak} > 10$ km s^{-1} and $v_{\rm max} > 7$ km s^{-1} samples in Table 3.

Via Lactea can also be used to extract the angular distribution of subhalos. This will be important for determining the errors on the overall satellite abundance that may arise from limited sky coverage. The SDSS DR5 footprint covers 8000 deg^2, or a fraction $f_{\rm DR5} = 0.194$ of the sky. While this is a sizable fraction of the sky, the top panel in Figure 4 shows that the subhalo distribution (projected out to the virial radius, in this case) is quite anisotropic, even on this scale. The color of each pixel is set by the fraction of all the subhalos, $f(<\Omega)$, that exist within an area of $\Omega_{\rm DR5} = 8000$ deg^2, centered on this pixel. We see clearly that the fraction of satellites within a DR5-sized region can vary considerably (from 0.12 to 0.28), depending on the pointing orientation. The same information is shown as a histogram in the bottom

panel, now presented as the implied multiplicative "sky coverage" correction factor, $c_\Omega = 1/f(<\Omega)$. Each of the 3096 pixels in the sky map is included as a single count in the histogram. Note that while the average correction factor is $c_\Omega = 1/f_{\rm DR5} = 5.15$ (as expected), the correction can vary from just $\sim$3.5 up to $\sim$8.3, depending on the mock survey's orientation.

Before moving on, we note that the expected anisotropy may contain a possible solution to the "missing inner satellites problem" described in Diemand et al. (2007a), which notes that there are $\sim$20 subhalos in Via Lactea within the innermost parts of the halo, while only a few galaxies are actually observed. While numerical effects may become important for these subhalos, given their sizes and how close they are to the center of the host, it may also simply be an observational coverage effect. If only subhalos within 23 kpc (the distance to Segue 1) are considered, $\sim$15% of the sky has one or zero subhalos visible in a survey the size of SDSS. This means that even if all of the subhalos host galaxies, there is a 15% chance that we will at most see a galaxy like Segue 1. The fact that Segue 1 was only recently discovered shows that there is easily room for a significant number of inner satellites that have gone as yet undetected simply because a survey like SDSS is necessary to uncover such objects, but over the entire sky instead of just a fifth.

2.4. *Observed Satellite Galaxies*

A variety of authors have identified dSph's in the DR5 footprint, including some that straddle the traditional boundaries between globular clusters and dSph's. For example, Willman 1 was originally of unclear classification (Willman et al. 2005), but is now generally recognized as being a dark matter–dominated dSph (Martin et al. 2007; Strigari et al. 2008b). Table 1 lists the complete set of dwarf galaxies from DR5 used in this analysis. For the SDSS dwarfs, we use the luminosities from Martin et al. (2008), which presents a homogeneous analysis, for all of the SDSS dwarfs, as well as de Jong et al. (2008) for Leo T, which is based on much deeper photometry. We note that these results are in generally good agreement with preexisting analyses (Willman et al. 2005; Belokurov et al. 2006; Simon & Geha 2007; Walsh et al. 2007, 2008). Here we also list the "classical" dwarfs, which were discovered before the SDSS, along with Segue 1, which was discovered from data for the SDSS-II SEGUE survey (Belokurov et al. 2007). All of the objects we list in this table have large mass-to-light ratios (Martin et al. 2007; Simon & Geha 2007; Strigari et al. 2008b).

For our fiducial corrections, following the convention of Koposov et al. (2008), we have not included Segue 1, as it does not lie inside the DR5 footprint and hence the published DR5 detection limits are not applicable. We do include Segue 1 in an alternative correction scenario below (see Table 3). We do not correct the classical dwarf satellite galaxies for luminosity bias or sky coverage, because appropriate detection limits for these classical dwarf satellites are unclear, given that they are not part of a homogeneous survey like SDSS. We assume that all satellites within those magnitude bins would have been discovered anywhere in the sky, with the possible exception of objects at low Galactic latitudes, where Milky Way extinction and contamination become significant (Willman et al. 2004a). This assumption is conservative in the sense that it will bias our total numerical estimate low, but it is only a minor effect, as our correction described in § 3 is dominated by low-luminosity satellites.

Before we use the radial distribution of Via Lactea subhalos to correct the observed luminosity function, it is important to investigate whether this assumption is even self-consistent with the data we have on the radial distribution of known satellites. The relevant comparison is shown in Figure 5. We have normalized to an outer radius $R_{\rm outer} = 417$ kpc (slightly larger than the Via Lactea virial radius) in order to allow a comparison that includes the DR5 dwarf Leo T; this extension is useful because the known dwarf satellite count is so low that even adding one satellite to the distribution increases the statistics significantly.

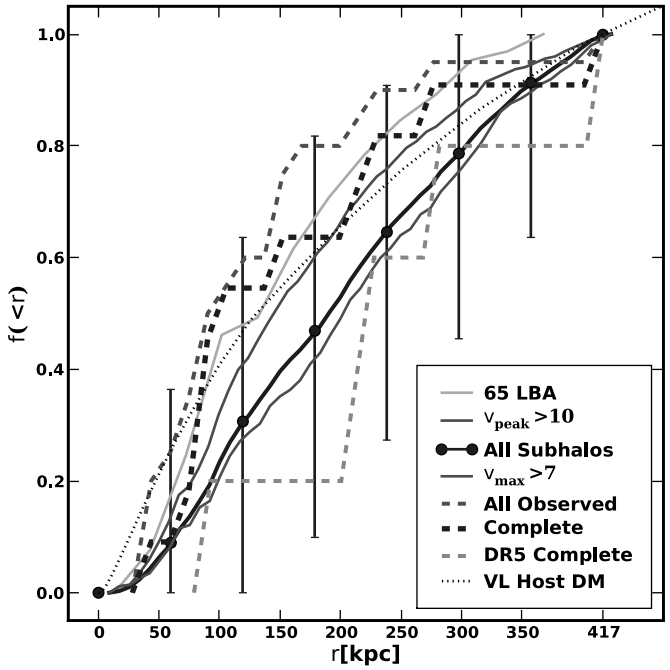

FIG. 5.—Radial distributions for various populations of observed satellites as compared to several sample subhalo distributions in Via Lactea. The solid lines show four populations of Via Lactea subhalos within 417 kpc: *top to bottom*, 65 largest before accretion (LBA; see Madau et al. 2008, their Fig. 7), $v_{\rm peak} > 10$ km s^{-1}, all (i.e., $v_{\rm peak} > 5$ km s^{-1}), and $v_{\rm max} > 7$ km s^{-1}. The dashed lines are observed satellite distributions: *top to bottom*, "All Observed" consists of all known Milky Way dSph satellites; the "Complete" distribution corresponds only to those with magnitudes corresponding to $R_{\rm comp} \geq 417$ kpc; "DR5 Complete" corresponds to satellites brighter than the completeness magnitude and also in the DR5 footprint; these are the only observationally complete and homogeneous sample. The dotted line is the global dark matter distribution for the Via Lactea host halo. Error bars (98% CL) are derived by randomly sampling from the Via Lactea subhalos the same number of satellites as in the "Complete" sample (11). Note that this means the error bars apply only to comparing the solid lines to the dashed line and that they are correlated, but still represent the scatter of individual bins in any possible observed sample of 11 satellites from Via Lactea. [*See the electronic edition of the Journal for a color version of this figure.*]

The radial distribution of all 23 known Milky Way satellites is shown by the dot-dashed line in Figure 5. The four solid lines show radial distributions for four choices of subhalo populations, the 65 largest $v_{\rm peak}$ (*upper solid line*) subhalos (65 LBA), as discussed in Madau et al. (2008), $v_{\rm peak} > 10$ km s^{-1} (*upper middle line*), $v_{\rm peak} > 5$ km s^{-1} (*lower middle line*), and $v_{\rm max} > 7$ km s^{-1} (*lower line*). We note that the all-observed profile is clearly more centrally concentrated than any of the theoretical subhalo distributions. However, as shown in Figure 1, our limited ability to detect faint satellite galaxies almost certainly biases the observed satellite population to be more centrally concentrated than the full population.

If we include only the 11 satellites (excluding SMC and LMC) that are bright enough to be detected within 417 kpc ($M_V \lesssim -7$), we obtain the thick dashed line. This distribution is significantly closer to all of the theoretical subhalo distributions and matches quite well within $r \sim 50$ kpc, where the incompleteness correction to the luminosity function will matter most. It is still more centrally concentrated than the distribution of all subhalos, however,

TABLE 2
K-S Test Results for Radial Distributions Shown in Figure 5

Distribution 1	Distribution 2	p-Value (%)
All observed	65 LBA	57.6
All observed	$v_{peak} > 10$	10.3
All observed	All subhalos	0.4
All observed	$v_{max} > 7$	0.1
Complete	65 LBA	95.1
Complete	$v_{peak} > 10$	38.2
Complete	All subhalos	12.1
Complete	$v_{max} > 7$	8.2
DR5 complete	65 LBA	8.6
DR5 complete	$v_{peak} > 10$	14.4
DR5 complete	All subhalos	48.2
DR5 complete	$v_{max} > 7$	63.1
All observed	Complete	87.6
All observed	DR5 complete	6.6
Complete	DR5 complete	41.1

as has been noted in the past (at least for the classical satellites; e.g., Willman et al. 2004b; Diemand et al. 2004; Kravtsov et al. 2004). In order to more rigorously determine whether the theoretical distribution is consistent with that of the 11 "complete" satellites, we have randomly determined the radial distribution of $v_{peak} > 5$ km s^{-1} subhalos using 1000 subsamples of 11 subhalos each. The error bars reflect 98% CL (confidence level) ranges from these subsamples, although they are correlated and hence represent only a guide to the possible scatter about the points in the distribution. From this exercise, we can roughly conclude that the complete observed distribution is consistent with being a random subsample of the $v_{peak} > 5$ km s^{-1} population. We also note that the $v_{peak} > 10$ km s^{-1} distribution fits even more closely, well within their 68% distribution (errors on this theoretical distribution are not shown for figure clarity, but they are similar in magnitude to those on the central line).

To further investigate the issue of consistency between the various radial distributions, we determine the Kolmogorov-Smirnov (K-S) probability for various distributions. The results are shown in Table 2, where in each case the p-value gives the probability that the null hypothesis is correct (i.e., that the two distributions are drawn from the same underlying distribution). While the distribution of all satellites is clearly inconsistent with the subhalo distributions, choosing only the complete satellites improves the situation, giving a reasonable probability of the complete distribution matching the $v_{peak} > 5$ km s^{-1} distribution and an even better match for the distributions that are cut on v_{peak}, as expected from the error bars.

Finally, we note that our definition of "complete" is conservative, since no satellites fainter than $M_V = -8.8$ were known before the SDSS survey. If we include only the (five) satellites bright enough to be detectable to R_{outer} that exist within the well understood area of the DR5 footprint, we obtain the radial profile shown by the dashed line in Figure 5 ("DR5 Complete"), which is even less centrally concentrated than any of the theoretical lines. While this distribution is marginally consistent with the other distributions based on the K-S test p-values, caution is noted, given the small number of data points (5). We conclude that while more data (from deeper and wider surveys) is absolutely necessary in order to determine the radial distribution of Milky Way satellites and to compare it with theoretical models, the assumption that the underlying distribution of satellites tracks that predicted for subhalos is currently consistent with the data. We adopt this assumption for our corrections below; specifically, we use the $v_{peak} > 5$ km s^{-1} distribution for our fiducial case. While the $v_{peak} > 10$ km s^{-1} distribution fits the observed satellites more closely, we show in § 3 that the various subhalo distributions affect only the final satellite counts by a factor of at most ~1.4. We chose to use all Via Lactea subhalos (corresponding to $v_{peak} > 5$ km s^{-1}) as our fiducial case in order to reduce statistical noise from the smaller number of satellites in the $v_{peak} > 10$ population; note that numerical effects will generally produce an undercorrection (giving a smaller number of satellites), as described in § 3.

Previous studies have pointed to discrepancies between simulations and observations of other galaxies' satellite distributions (e.g., Diemand et al. 2004; Chen et al. 2006). While this is of concern, many of these data are around clusters or other environments very different from that of the Local Group. Furthermore, the detection prospects for faint satellites around the Milky Way are of course far better than can be achieved for other galaxies, and the region of the luminosity function that is of importance for this correction (e.g., $M_V > -7$) has never been studied outside the Local Group.

3. LUMINOSITY FUNCTION CORRECTIONS

The cumulative number of known Milky Way satellites brighter than a given magnitude is shown by the lower dashed line with filled circles in Figure 6. This luminosity function includes both the classical dwarf satellites and the fainter, more recently discovered SDSS satellites (excluding Segue 1 for reasons discussed above). By simply multiplying the SDSS satellite count by the inverse of the DR5 sky fraction ($1/f_{DR5}$) and adding this to the classical dwarf satellite count, we produce the long-dashed line. This first-order correction provides an extremely conservative lower estimate on the total Milky Way satellite count by ignoring the details of luminosity bias in the SDSS.

We use the following series of mock surveys of the Via Lactea subhalo population in order to provide a more realistic correction. First, an observer is positioned at distance of 8 kpc from the center of Via Lactea. We then define an angular point on the sky from this location and use it to center a mock survey of solid angle $\Omega_{DR5} = 8000$ deg^2. We allow this central survey position to vary over the full sky using 3096 pointings that evenly sample the sky. Although we find that the absolute position of the observer does not affect our results significantly, we also allow the observer's position to vary over six specific locations, at $(x, y, z) = (\pm 8, 0, 0)$, $(0, \pm 8, 0)$, and $(0, 0, \pm 8)$ on the Via Lactea grid. We acknowledge that there are (contradictory) claims in the literature concerning whether satellite galaxies are preferentially oriented (either parallel or perpendicular) with respect to galaxy disks (Kroupa et al. 2005; Metz et al. 2007; Kuhlen et al. 2007; Wang et al. 2008; Faltenbacher et al. 2008) and equally contradictory claims regarding how disks are oriented in halos (Zentner et al. 2005; Bailin et al. 2005; Dutton et al. 2007). If there were a preferential orientation, then the appropriate sky coverage correction factors would need to be biased accordingly, but for our correction, we make no assumptions about the orientation of the "disk." Therefore, any uncertainty in the correct orientation of the disk is contained within the errors we quote on our counts. In the end, we produce 18,576 equally likely mock surveys, each with their own correction factors, and use these to correct the Milky Way satellite luminosity function for angular and radial incompleteness.

For each of the mock surveys, we consider every DR5 satellite ($i = 1, \ldots, 11$, sometimes 12) with a heliocentric distance within $R_{outer} = 417$ kpc and determine the total number of objects of its

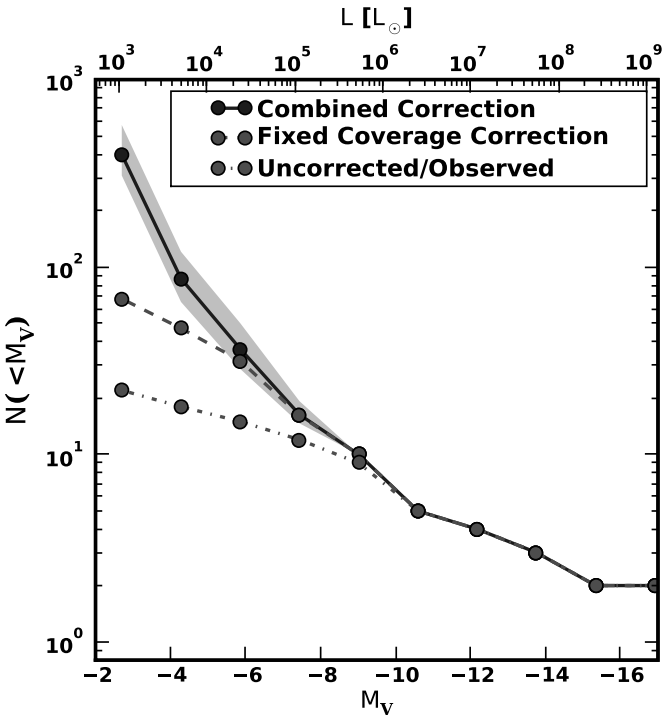

FIG. 6.—Luminosity function as observed (*lower curve*), corrected only for SDSS sky coverage (*middle curve*), and with all corrections included (*upper curve*). Note that the classical (pre-SDSS) satellites are uncorrected, while new satellites have the correction applied. The shaded error region corresponds to the 98% spread over our mock observation realizations. Segue 1 is not included in this correction. [*See the electronic edition of the Journal for a color version of this figure.*]

luminosity that should be detectable. Specifically, if satellite i has a magnitude M_V^i that is too faint to be detected at $R_{\rm outer}$ (i.e., if $M_V^i \gtrsim -7$), then we determine the number of Via Lactea subhalos, $N(r < R_{\rm comp},\ \Omega < \Omega_{\rm DR5})$, that are situated within an angular cone of size $\Omega_{\rm DR5}$ and within a heliocentric radius $R_{\rm comp}(M_i)$. We then divide the total number of Via Lactea subhalos, $N_{\rm tot}$ by this "observed" count and obtain a corrected estimate for the total number satellites of magnitude M_V^i:

$$c^i = \frac{N_{\rm tot}}{N(r < R_{\rm comp}(M_V^i),\ \Omega < \Omega_{\rm DR5})}. \tag{3}$$

If the SDSS satellite i is bright enough to be seen at $R_{\rm outer}$, then $R_{\rm comp}$ is replaced by $R_{\rm outer}$ in equation (3). In this case, the correction factor accounts only for angular incompleteness. This method allows us to produce distributions of correction factors for each M_V of relevance. Note also that because the correction factor is the fraction of subhalos in the cone, it depends only on the distributions of Via Lactea subhalos, rather than directly depending on the total number, rendering it insensitive to the overall subhalo count in Via Lactea. Furthermore, any subhalo distributions that do not have enough subhalos to fully accommodate all possible pointings are simply given the correction factor $1/N_{\rm tot}$, meaning that numerical effects tend to *under*correct, producing a conservative satellite estimate.

Three example distributions of number count correction factors are shown in Figure 7 for hypothetical objects of luminosity $M_V = -3$, -5, -7 and corresponding completeness radii $R_{\rm comp} = 77$, 194, and 486 kpc. We see that while the brightest objects typically have correction factors of order the inverse of the sky coverage fraction, $\sim$5, the faintest objects can be undercounted by a factor of $\sim$100 or more. Note that to produce heliocentric sky coverage maps, we must assume a plane in Via Lactea in which we consider the Sun to lie; for Figure 7, this is the xy-plane, but for our final corrections we consider all possible orientations (described above).

We construct corrected luminosity functions based on each of the 18,576 mock surveys by generating a cumulative count of the observed satellites. We weight each satellite i by its associated correction factor c^i and (in our fiducial case) its detection efficiency ϵ^i. For each of the new satellites we use the quoted detection efficiencies from Koposov et al. (2008, their Table 3). We reproduce those efficiencies in our Table 1, and we assume $\epsilon = 1$ for all of the classical satellites that are not within the DR5 footprint. Explicitly, the cumulative luminosity function for a given pointing is

$$n(< M_V) = \sum_i^{<M_V} \frac{c(M_V^i)}{\epsilon^i}. \tag{4}$$

For a given scenario (subhalo population, completeness limits, and detection efficiencies for each satellite), we determine the luminosity function for each pointing and disk orientation. We are then able to calculate a median luminosity function and scatter for each scenario.

Our fiducial corrected luminosity function shown by the upper solid line in Figure 6, and the shaded band spans the 49% tails of the distribution. Note that the errors vanish around $M_V = -9$, because all satellites brighter than that are "classical" pre-SDSS satellites and are left completely uncorrected on the conservative assumption that any objects brighter than this would have been detected previously. Our fiducial scenario counts galaxies within a radius $R_{\rm outer} = 417$ kpc and excludes Segue 1 from the list of corrected satellites, because it is not within the DR5 footprint. In addition, this scenario uses quoted detection efficiencies ϵ from Koposov et al. (2008) and the completeness radius relation in equation (2) with $a = 0.6$ and $b = 5.23$. With this fiducial scenario, we find that there are 398^{+178}_{-94} (98% CL) satellites brighter than Boo II within 417 kpc of the Sun.

We have performed the same exercise for a number of different scenarios as described in Table 3 and summarized in Figure 8. Table 3 assigns each of these scenarios a number (col. [1]) based on different assumptions that go into the correction. Scenario 1 is our fiducial case and counts all satellites brighter than Boo II ($M_V > -2.7$) within $R_{\rm outer} = 417$ kpc. Scenario 2 counts the total number of satellites brighter than Segue 1 ($M_V > -1.5$) if we consider Segue 1 as included in the DR5 sample (col. [5]). Scenarios 3–4 exclude Boo II or Willman 1 (the faintest satellites) along with Segue 1, considering the possibility that these satellites are low luminosity because of strong environmental effects or are not even truly dwarf galaxies at all. Alternatively, scenario 4 may be considered the total number brighter than Coma (the fourth faintest). Scenarios 5–10 allow for different choices within the Via Lactea subhalo population (col. [7]), and scenarios 11–14 reflect changes in outer Milky Way radius, $R_{\rm outer}$ (col. [4]). Scenarios 16–17 allow different values for a and b in equation (2) (specified in cols. [2] and [3]) for the $R_{\rm comp}(M_V)$ relation, and scenario 15 assumes that the detection efficiency for all satellites is $\epsilon = 1$. Finally, scenario 18 makes the extreme assumption that there is no luminosity bias and includes only a sky coverage correction factor. In cols. [8]–[10], $N_{\rm sats}$ is the number of satellites expected for a given scenario, while $N_{\rm upper}$ and $N_{\rm lower}$ are the upper and lower limits for the 98% distribution. The final column gives the faint-end (i.e., $-2 \gtrsim M_V \gtrsim -7$) slope if the luminosity function is approximated by the form $dN/dL_V \sim L^\alpha$. Note that some

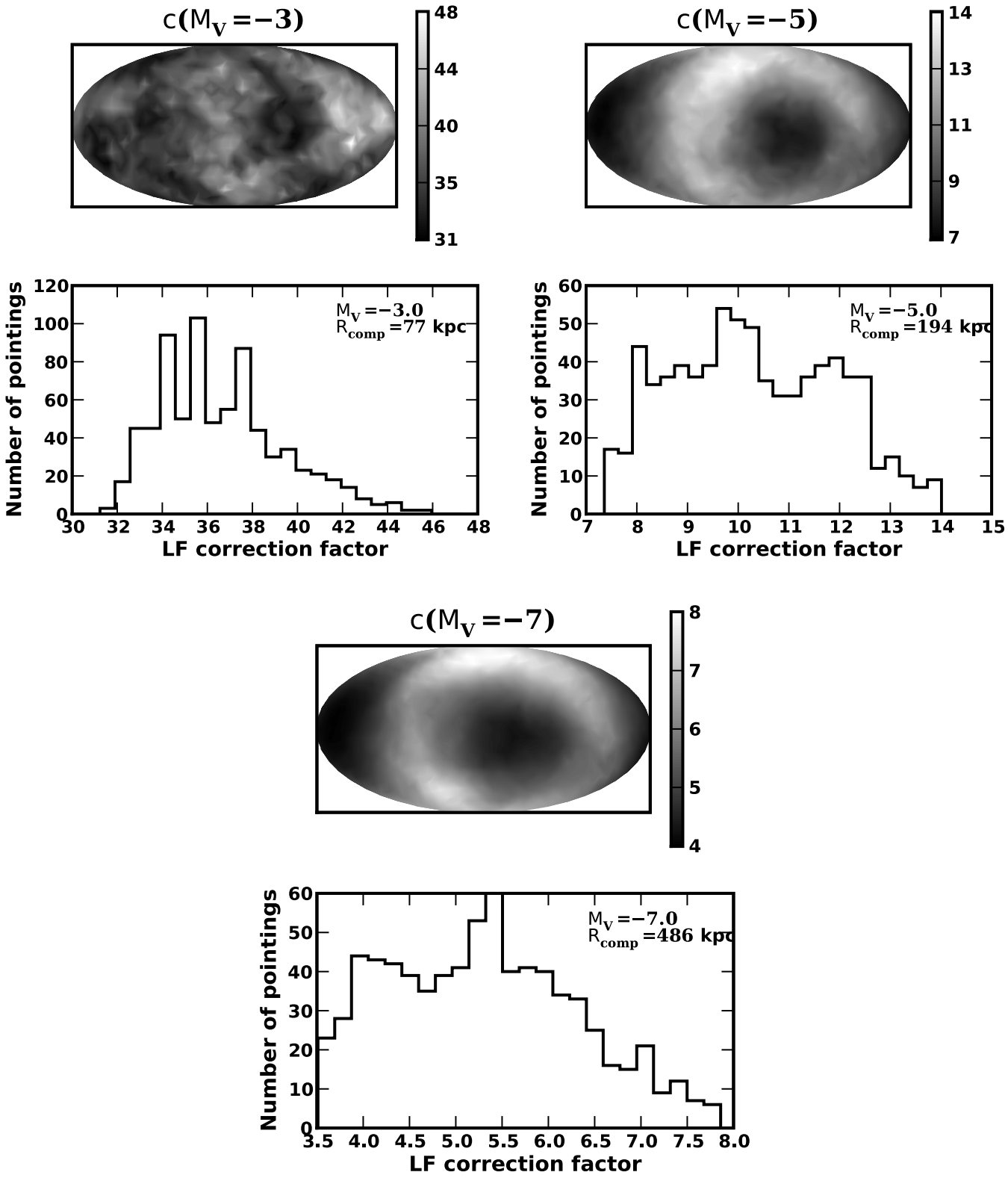

FIG. 7.—Sky anisotropy maps and corresponding distributions for three sample limiting magnitudes. The sky projections are the corresponding correction factor (i.e., the inverse of the enclosed fraction of total satellites) for a DR5-sized survey pointing in a given direction corresponding to a satellite of a particular magnitude. The histograms show the distribution of correction factors from evenly sampling the sky maps. *Top to bottom*: Limiting magnitudes $M_V = -3$, -5, and -7, corresponding to $R_{\rm comp} = 77$, 494, and 486 kpc. [*See the electronic edition of the Journal for a color version of this figure.*]

of these luminosity functions are *not* consistent with a power law within the anisotropy error bars, but we include the best fits for completeness (see § 6 for further discussion).

From Figure 8, for all of the cases that adopt the fiducial detection limits (scenarios 1–15), we may expect as many as ~500 satellites within ~400 kpc. Even the most conservative completeness scenarios (4, 10, 11, and 14) suggest that ~300 satellites may exist within the Milky Way's virial radius. Scenario 17, which relies on a less conservative, but not unreasonable, detection limit, suggests that there may be more than ~1000 Milky

TABLE 3
RESULTS OF LUMINOSITY FUNCTION CORRECTION

Scenario (1)	a (2)	b (3)	R_{outer} (kpc) (4)	Excluded Satellites (5)	Detection Effeciency (6)	Subhalos (7)	N_{sats} (8)	N_{upper} (9)	N_{lower} (10)	Faint-End Slope (α) (11)
1	−0.600	−0.719	417	Seg1	Yes	All	398	576	304	-1.87 ± 0.19
2	−0.600	−0.719	417	None	Yes	All	558	881	420	-1.78 ± 0.20
3	−0.600	−0.719	417	Seg1, BooII	Yes	All	328	561	235	-1.47 ± 0.18
4	−0.600	−0.719	417	Seg1, BooII, Wil1	Yes	All	280	505	194	-1.66 ± 0.17
5	−0.600	−0.719	417	Seg1	Yes	$v_{max} > 5$	464	749	316	-1.92 ± 0.23
6	−0.600	−0.719	417	Seg1	Yes	$v_{max} > 7$	427	942	258	-1.90 ± 0.32
7	−0.600	−0.719	417	Seg1	Yes	$v_{peak} > 9$	302	508	198	-1.90 ± 0.42
8	−0.600	−0.719	417	Seg1	Yes	$v_{peak} > 10$	289	521	191	-1.76 ± 0.29
9	−0.600	−0.719	417	Seg1	Yes	$v_{peak} > 14$	260	531	167	-1.72 ± 0.32
10	−0.600	−0.719	417	Seg1	Yes	65 LBA	224	752	128	-1.67 ± 0.44
11	−0.600	−0.719	200	Seg1	Yes	All	229	330	176	-1.70 ± 0.18
12	−0.600	−0.719	300	Seg1	Yes	All	322	466	246	-1.80 ± 0.19
13	−0.600	−0.719	389	Seg1	Yes	All	382	554	292	-1.87 ± 0.19
14	−0.600	−0.719	500	Seg1	Yes	All	439	637	335	-1.89 ± 0.20
15	−0.600	−0.719	417	Seg1	No	All	184	259	142	-1.65 ± 0.19
16	−0.684	−0.753	417	Seg1	Yes	All	509	758	381	-1.95 ± 0.20
17	−0.667	−0.785	417	Seg1	Yes	All	1093	2261	746	-2.15 ± 0.26
18	...	...	417	Seg1	...	All	69	100	50	-1.16 ± 0.21

NOTES.—The last four columns provide median, upper, and lower estimates (98% range) for the Milky Way satellite count within R_{outer}, as well as the faint-end slope (as the Schechter α, i.e., $dN/dL_V \propto L_V^{\alpha}$) for several different scenarios. See text for a description.

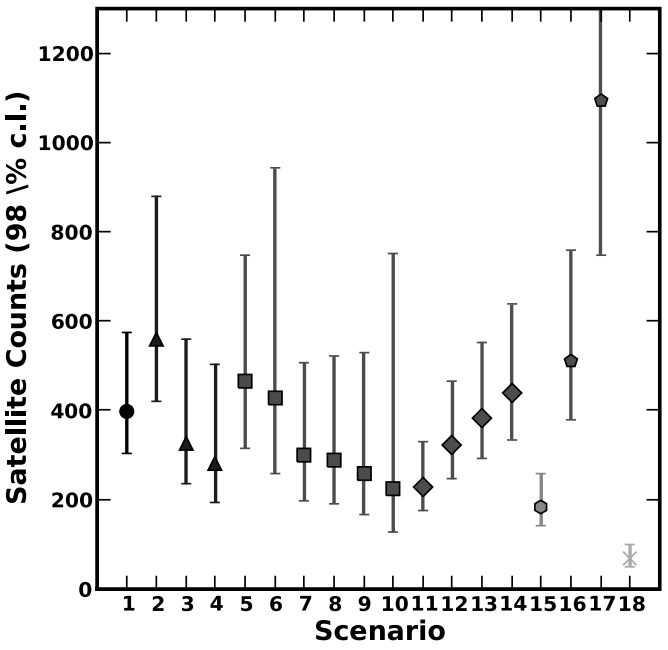

FIG. 8.—Number of Milky Way satellites for several different scenarios as described in Table 3. Error bars reflect 98% ranges about the median values (*points*). Scenario 1 (*circle*) is our fiducial case and counts all satellites brighter than Boo II ($M_V > -2.7$) within $R_{outer} = 417$ kpc. Scenarios 2–4 (*triangles*) consider inclusion or exclusion of different satellites. Scenarios 5–10 (*squares*) allow for different choices within the Via Lactea subhalo population, scenarios 11–14 (*diamonds*) reflect changes in R_{outer}, scenario 15 (*hexagon*) corresponds to no detection efficiency correction, and scenarios 16 and 17 (*pentagons*) are for different completeness limit assumptions. Scenario 18 (*cross*) includes only the angular (sky coverage) correction factor, i.e., no luminosity bias correction. [*See the electronic edition of the Journal for a color version of this figure.*]

Way satellites waiting to be discovered. We now turn to a discussion of the prospects for this exciting possibility.

4. PROSPECTS FOR DISCOVERY

Upcoming large-area sky surveys such as LSST, DES, Pan-STARRS, and SkyMapper (Ivezic et al. 2008; Frieman et al. 2005; Kaiser et al. 2002; Keller et al. 2007), will survey more sky and provide deeper maps of the Galactic environment than ever before possible. In this section we provide a first rough estimate for the number and type of satellite galaxies that one may expect to discover with these surveys.

While it is impossible to truly ascertain the detection limits without detailed modeling and consideration of the sources of contamination for the magnitudes and colors these surveys will probe, the simplest approximation is to assume that all the characteristics of detectability are the same as those for SDSS, aside from a deeper limiting magnitude. If we do this, we can estimate the corresponding completeness radius for each survey by the difference between the limiting (5 σ) r-band point-source magnitude for Sloan ($M_{SDSS} = 22.2$) and the corresponding limit for the new survey:

$$\frac{R_{comp}^{lim}}{R_{comp}^{SDSS}} = 10^{(M_{lim}-M_{SDSS})/5}. \quad (5)$$

Figure 9 shows the results of this exercise for several planned surveys. According to this estimate, LSST, with a co-added limit of $M_{LSST} = 27.5$, should be able to detect objects as faint as the faintest known galaxies out to the Milky Way virial radius. Moreover, LSST will be able to detect objects as faint as $L \sim 100\,L_{\odot}$ (if they exist) out to distances of $\sim$200 kpc.

Examining the prospects for dwarf satellite detection with LSST in more detail, in Figure 10 we plot the number of satellites that LSST would detect in 4π sr, assuming that the true satellite distribution follows that expected from our fiducial correction presented above. Remarkably, even with single-exposure coverage (to 24.5), LSST will be able to discover a sizable fraction of the

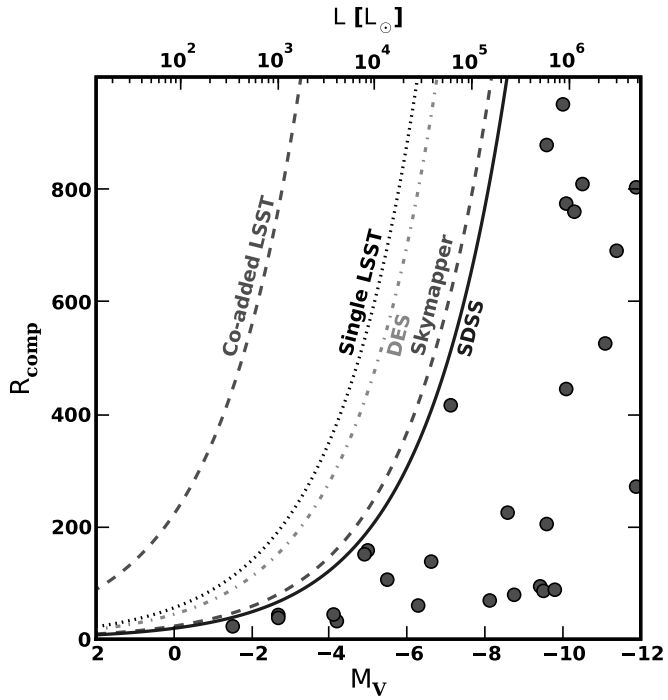

FIG. 9.—Maximum radius for detection of dSph's as a function of galaxy absolute magnitude for DR5 (assumed a limiting r-band magnitude of 22.2) compared to a single exposure of LSST (24.5), co-added full LSST lifetime exposures (27.5), DES or one exposure from PanSTARRS (both 24), and the SkyMapper and associated Missing Satellites Survey (22.6). The data points are SDSS and classical satellites, as well as Local Group field galaxies. [*See the electronic edition of the Journal for a color version of this figure.*]

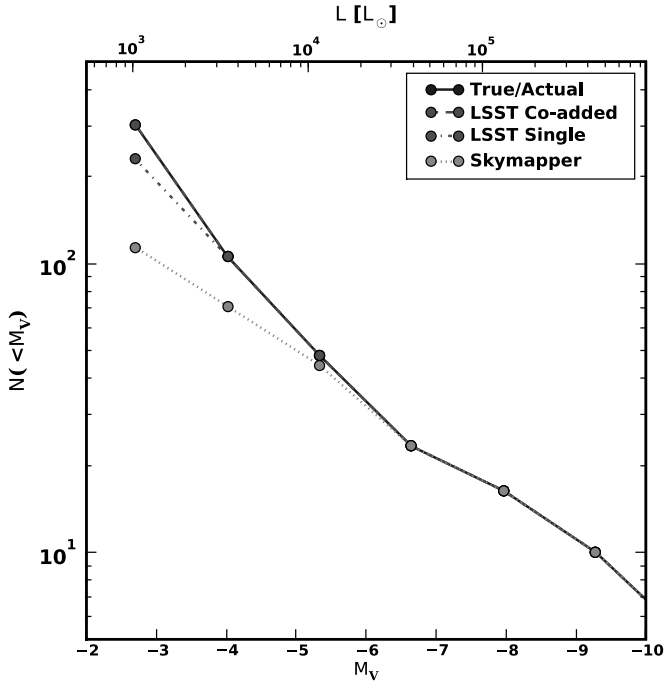

FIG. 10.—Expected luminosity functions for LSST per 4π sr. For the single exposure, the adopted limiting magnitude is $r_{\rm lim} = 24.5$, while for the co-added case, $r_{\rm lim} = 27.5$ The Skymapper curve assumes a hypothetical full sky coverage survey of the same limiting magnitude as Skymapper ($r_{\rm lim} = 22.6$). [*See the electronic edition of the Journal for a color version of this figure.*]

TABLE 4

PREDICTED NUMBER OF DETECTABLE SATELLITES IN A SERIES OF UPCOMING SURVEYS

Survey	Area (deg^2)	Limiting r (mag)	$N_{\rm sats}$
RCS-2	1000	24.8	3–6
DES	5000	24	19–37
Skymapper	20000	22.6	42–79
PanSTARRS 1	30000	22.7	61–118
LSST 1-exp	20000	24.5	93–179
LSST combined	20000	27.5	145–283

NOTE.—Crowding and confusion effects, which will reduce the number of detections of faint objects, have been ignored.

satellites in the Southern sky, >100 galaxies by this estimate. Moreover, the co-added data would reveal all ~180 dwarf galaxies brighter than Boo II (and perhaps even more if they exist at lower luminosities). A survey such as this will be quite important for testing galaxy formation models, as even the shape of the satellite luminosity function is quite poorly constrained. In Figure 10, the Skymapper line appears close to a power law over the range shown, while the "actual" luminosity function is certainly not.

Finally, in Table 4, we present predictions for the number of satellites that will be found in each of a series of upcoming large-area surveys, as well an example smaller scale survey, RCS-2 (Yee et al. 2007). Given their limiting magnitudes and their fractional sky coverage and assuming the fiducial scenario outlined above, we can essentially perform the inverse of the correction described in § 3 and determine the number of satellites the survey will detect (as done in Fig. 10 for LSST). Note that this still ignores more complicated issues such as background galaxy contamination and problems with stellar crowding, which are potentially serious complications, particularly for the faintest of satellites. Hence, these estimates are upper limits, but to first order they are a representative number of the possibly detectable satellites given the magnitude limits and sky coverage. Some of the footprints of these surveys will overlap, however, which will improve the odds of detection, but reduce the likely number of new detections for later surveys (this effect is not included in the counts in Table 4).

5. DISCUSSION

5.1. *Caveats*

While our general expectation that there should be many more satellites seems to be quite solid, there are several important caveats that limit our ability to firmly quote a number or to discuss the expected overall shape of the luminosity function.

1. *Detection limits*.—The simplifying approximation that equation (1) describes the complexities of satellite detection cannot be correct in detail; we expect a dependence on properties such as Galactic latitude and color. However, we are leaving these issues aside for this first-order correction. Moreover, the detection limits from Koposov et al. (2008) apply only to objects with surface brightness $\mu_V \lesssim 30$; if dSph's more diffuse than this exist, they will have been missed by SDSS. In this sense, our results are conservative, as even more very low surface brightness dwarf galaxies may be discovered by new, deeper surveys.

2. *Input assumption*.—The assumption that the satellite population tracks the full underlying subhalo population is a major assumption of this correction. As Figure 5 shows, this assumption

is consistent with the current data, and modest cuts on v_{peak} improve the situation further. Given the size of the error bars, the existence of a discrepancy simply cannot be resolved without surveys that have better completeness limits. There are certainly reasons to expect that the satellite population *will not* track the subhalo population in an unbiased way, for example, if tidal forces play a role in making ultrafaint dSph galaxies. However, there are also reasons to suspect that there is no such bias. The dark matter subhalo masses of the known Milky Way dwarfs are approximately the same over a $\sim$4 orders-of-magnitude spread in luminosity (Strigari et al. 2008a, 2008b), suggesting that the luminosity that any subhalo obtains is quite stochastic. Whether or not our input assumption about galaxies tracing subhalos is correct, future surveys will provide a means to test it and thereby provide an important constraint on the formation processes of these extreme galaxies.

3. *Subhalo distribution*.—Our correction relies on the Via Lactea subhalo population and its distribution with radius and angle. While this provides a well-motivated starting point for this correction, Via Lactea is only a single realization of a particular mass halo and of a particular set of cosmological parameters (*WMAP* 3 yr) and hence cannot necessarily be considered representative of a typical halo in ΛCDM. Semianalytical models suggest that the cosmic variance in radial distributions should not be very large, as long as we consider subhalos that are small enough that the mass function is well populated (Zentner & Bullock 2003). However, a suite of Via Lactea–type simulations will be necessary to produce a distribution of corrections to statistically average over before this correction can be considered fully numerically robust. As discussed in § 1, the uncertainty in the properties of the Milky Way halo also mean that using Via Lactea to accurately model the Milky Way is subject to those same uncertainties. This uncertainty is alleviated in this correction because only the fraction distribution matters; the absolute normalization is determined by the *observed* satellites, rather than the subhalo counts. But if it is true that the radial distribution of subhalos tracks the global dark matter distribution, as suggested by Diemand et al. (2007b) and Figure 3, this uncertainty could be important if the inner portions of the radial distribution change substantially with cosmological parameters or halo properties.

Note that while the mass of Via Lactea is quite close to that obtained from ΛCDM-based mass models of the Milky Way (e.g., Klypin et al. 2002; Madau et al. 2008), the mass of the Milky Way halo is constrained by observations only at the factor of $\sim$2 level. The most relevant uncertainty associated with the possible mass difference between the Milky Way and Via Lactea is the difference associated with the uncertain radial scaling. Since $R_{200} \propto M_{200}^{1/3}$, a factor of $\sim$2 mass uncertainty corresponds to a $\sim\pm25\%$ uncertainty in virial radius. Fortunately, our corrections depend primarily on the relative radial distribution of satellites, not on their absolute masses, and the choice of exactly what radius within which galaxies are considered "satellites" is somewhat arbitrary, anyway. Moreover, the expected subhalo angular anisotropy (see § 3) is more important for our corrections than the uncertainty associated with the Milky Way halo mass or precisely how the outer radius is defined.

4. *Input luminosities/satellites*.—Most of our corrections come from the faintest nearby satellites, as they have very small R_{comp} values compared to R_{outer}. Errors in the magnitudes of these faintest of satellites will result in significant changes in the derived luminosity function. These errors are not propagated for this correction, but revisions to faint satellite magnitudes have the potential to significantly alter our estimates. Furthermore, the final count is highly sensitive to Poisson statistics in the innermost regions of the Milky Way, as well as any physical effect that biases the radial distribution of the faintest of the satellites (as discussed above).

5.2. *Implications*

Keeping in mind the caveats discussed above, it is worth considering the potential implications of a Milky Way halo filled with hundreds of satellite galaxies. For the sake of discussion, we adopt $N_{sat} \simeq 400$, as obtained in our fiducial estimate.

First, $N_{sat} \simeq 400$ can be used to determine a potential characteristic velocity scale in the subhalo distribution. Under the (extreme) assumption that only halos larger than a given velocity host satellites, Figure 2 implies that $N \simeq 400$ corresponds to a circular velocity $v_{max} \gtrsim 7$ km s^{-1} or a historical maximum of $v_{peak} \gtrsim 12$ km s^{-1}. We note that these cutoffs correspond closely to those adopted in our corrections (Table 3) and that there was no reason that they had to match. If we iteratively apply the correction in order to obtain perfect self-consistently between the corrected count and the input total, we find $v_{peak} > 14$ km s^{-1}. Interestingly, this scale is quite close to the threshold where gas may be boiled out of halos via photoevaporation (Barkana & Loeb 1999). We note, however, that the subhalo abundance at fixed mass or v_{max} may vary perhaps at as much as the factor of $\sim$2 level from halo to halo (Zentner & Bullock 2003). Therefore the "cosmic variance error" will affect our ability to determine a characteristic subhalo mass based on counts (but does not affect the correction itself, which depends only on the radial distribution, not the total counts of subhalos). Recently, Diemand et al. (2008) have published results from the Via Lactea II halo, which has a factor of $\sim$1.7 times more subhalos at fixed v_{max} than the Via Lactea halo we analyze here. If we take the velocity function in Diemand et al. (2008, their Fig. 3), N_{sat} would correspond to $v_{max} \gtrsim 9$ km s^{-1}.

While the maximum circular velocity of a subhalo is a useful measure of its potential well depth, it is very difficult to measure v_{max} directly from dwarf satellite stellar velocities (Strigari et al. 2007b). The best-determined dark halo observable is the integrated mass within a fixed radius within the stellar distribution (Strigari et al. 2007a). While the observed half-light radii vary from tens to hundreds of parsecs for the dwarf satellites, all dwarf satellites are found to have a common mass scale of $\sim 10^7\ M_\odot$ within a fixed radius of 300 pc within their respective centers (Strigari et al. 2008a) and to a similar extent a common mass of 10^6 within 100 pc (Strigari et al. 2008b). Although the masses within these scales are difficult to resolve with the Via Lactea simulation we consider in this paper, this mass scale will be well-resolved in Via Lactea II (Diemand et al. 2008) and forthcoming simulations. In the future, a statistical sample of highly resolved subhalos will allow for a robust comparison between the dwarf satellite mass function and the subhalo population. This in turn will allow corrections of the sort presented in this paper on various subpopulations of subhalos and galaxies, providing a much more stringent consistency check between the mass function and luminosity function in ΛCDM-based models. It is important to note, however, that the observed stellar kinematics of the satellites does set stringent limits on their host halo v_{max} values. These limits are consistent with the results presented here in that any of the reasonable subpopulations discussed above (e.g., $v_{max} \gtrsim 7$; 10 km s^{-1}) are not excluded by the current data (Strigari et al. 2007b, 2008b). We note that strong CDM priors suggest somewhat *larger* v_{max} values ($\gtrsim$15 km s^{-1}; Strigari et al. 2007b, 2008b; Peñarrubia et al. 2008), which would (if anything) *underpredict*

the observed visible satellite counts, according to our estimates. As we have shown, we expect the discovery of many more dwarfs to occur with planned surveys like LSST, DES, PanSTARRS, and SkyMapper. If so, it will provide important constraints on galaxy formation models, which at present are only poorly constrained by the present data. The ability to detect galaxies as faint as $L \sim 100\,L_{\odot}$ provides an opportunity to discover if there is a low-luminosity threshold in galaxy formation and to use these faint galaxies as laboratories to study galaxy formation in the extreme. The planned surveys will also provide an important measurement of the radial distribution of faint satellites. This will help test our predictions, but more importantly provide constraints on more rigorous models aimed at understanding why and how low-mass galaxies are so inefficient at converting their baryons into stars.

Another important direction to consider is searches for similar satellites around M31. New satellites are rapidly being discovered in deep surveys of its environs (e.g., McConnachie et al. 2008). While there are indications of substantial differences in the M31 satellites and their distributions compared to the Milky Way (McConnachie & Irwin 2006), such comparisons are complicated by the fact that it is impossible to detect the ultrafaint satellites that make up most of our corrected satellite counts at the distance of M31. With the much larger data samples that will be available with future deep surveys, it may be easier to compare the true luminosity function and distributions of Milky Way satellites to M31 and hence better understand the histories of both the galaxies, as well as better constrain how dSph's form in a wider ΛCDM context.

Finally, if LSST and other surveys do discover the (full sky) equivalent of ∼400 or even ∼1000 satellites and appropriate kinematic follow-up with 30 m–class telescopes like the Thirty Meter Telescope (TMT) confirms that these objects are indeed dark matter dominated, then it will provide a unique and powerful means to constrain the particle nature of dark matter. As discussed in § 1, the mass function of dark matter subhalos is expected to rise steadily to small masses as $\sim 1/M$ (Klypin et al. 1999; Diemand et al. 2007a), and the only scale that is expected to break this rise is the cutoff scale in the clustering of dark matter. When the MSP was originally formulated, scenarios like warm dark matter (WDM) were suggested as a means of "erasing" all but the ∼10 most massive subhalos per galaxy by truncating the power at $\sim 10^8\,M_{\odot}$ scales. If ∼1000 satellites were discovered, then the same idea could be used to provide a limit on the small-scale clustering characteristics of the dark matter particle. As a rough approximation, $N \simeq 1000$ subhalos corresponds to a minimum mass subhalo in Via Lactea of $M \simeq 10^7\,M_{\odot}$ (Diemand et al. 2007a), or an original mass (before infall) of $M_i \simeq 3 \times 10^7\,M_{\odot}$ (Diemand et al. 2007b). If we associate this $z = 0$ subhalo mass with a limiting free-streaming mass, then we obtain the bound $m_{\nu} \gtrsim 10$ keV on the sterile neutrino (Abazajian & Koushiappas 2006). This limit is competitive with the best constraints possible with the Lyα forest and is not subject to the uncertainties of baryon physics. Of course, WDM simulations will be required in order to convincingly make a link between satellite counts and the small-scale power spectrum, but these simulations are certainly viable within the time frame of LSST.

6. CONCLUSIONS

The goal of this paper has been to provide reasonable, cosmologically motivated corrections to the observed luminosity function. Our primary aim is to motivate future searches for faint dwarf galaxies and to explore the status of the missing satellites problem in light of the most recent discoveries. By combing completeness limits for the SDSS (Koposov et al. 2008) with the spatial distribution of subhalos in Via Lactea, we have shown that there are likely between ∼300 and ∼600 satellites brighter than Boo II within the Milky Way virial radius (Fig. 6) and that the total count may be as large as ∼2000, depending on assumptions (Table 3; Fig. 8). We also showed that the observed satellites are indeed consistent with tracing the radial distribution of subhalos, provided completeness limits are taken into account (Fig. 5; Table 2). Moreover, we argued that future large sky surveys like LSST, DES, PanSTARRS, and SkyMapper should be able to see these satellites if they do exist and thereby provide unprecedented constraints on the nature of galaxy formation in tiny halos.

While this correction predicts that nearly all of the undetected satellites are faint ($M_V > -7$) and consequently have low surface brightness, it is important to note that it is not clear how this maps onto satellites' $v_{\rm max}$. While a possible test of this correction's result lies in selecting subsamples of the observed satellite population, $v_{\rm max}$ is difficult to constrain in the known satellites (Strigari et al. 2007b), and hence this exercise is suspect until simulations can resolve subhalos well enough to compare to observables such as the integrated mass within 300 pc (see § 5.2).

There are two major points to take away from this correction:

1. As it was first formulated, the MSP referred to the mismatch between the then ∼10 known dwarf satellite galaxies of the Milky Way and Andromeda, and the expected count of ∼100–500 subhalos with $v_{\rm max} \geq 10\ {\rm km\ s^{-1}}$ (Klypin et al. 1999; Moore et al. 1999). Our results suggest that the recent discoveries of ultrafaint dwarfs about the Milky Way are consistent with a total population of ∼500 satellites, once we take into account the completeness limits of the SDSS. In this sense, the primary worries associated with the MSP in CDM are alleviated. Nonetheless, it is critical that searches for these faint galaxies be undertaken, as the assumptions of this correction must be tested.

2. The shape of the faint end of the satellite luminosity function is not yet constrained well enough to deeply understand the theoretical implications. There still exists a large parameter space in galaxy formation theory that will fall inside the error bars of Figure 6, and an even larger parameter space of models that are viable if our caveats and scenario possibilities are considered. Our results strongly suggest that the luminosity function continues to rise to the faint end, with a faint-end slope in our fiducial scenario given by $dN/dM_V = 10^{(0.35\pm0.08)M_V+3.42\pm0.35}$, or $dN/dL_V \propto L^{\alpha}$, with $\alpha = -1.9 \pm 0.2$. This is substantially steeper than the result of Koposov et al. (2008), possibly the result of using a ΛCDM-motivated subhalo distribution instead of the analytic profiles used in that paper. But caution is advised in reading anything into the details of the shape, as nearly anything could be hiding within the faintest few bins when all the scenarios are considered. This is apparent from Figure 10, where the Skymapper line appears as a power law over the range shown, while the actual luminosity function is certainly not. Furthermore, depending on which scenario is used, the slope (α) can vary anywhere from −1.16 to −2.15 (see col. [11] in Table 3).

Fortunately, future deep large sky surveys will detect very faint satellites out to much larger distances and hence firmly observe the complete luminosity function out beyond the Milky Way virial radius (see § 4). With these data, it will be possible to provide stringent limits both on cosmology and galaxy formation scenarios (see § 5.2). Nonetheless, the current data are not deep enough, and until the new survey data are available, there will be no way to put the specter of the MSP completely to rest.

We wish to acknowledge the creators of the Via Lactea Simulation and the public data release thereof (http://www.ucolick.org/~diemand/vl/data.html). We thank Manoj Kaplinghat, Betsy Barton, Anatoly Klypin, Jürg Diemand, Piero Madau, Ben Moore, Andrew Zentner, Nicolas Martin, and Alan McConnachie for helpful conversations and suggestions, as well as Brant Robertson for conversations and bringing the RCS-2 survey to our attention. We would also like to thank the anonymous referee for helpful comments and suggestions. This work was supported by the Center for Cosmology at UC Irvine.

REFERENCES

Abazajian, K., & Koushiappas, S. M. 2006, Phys. Rev. D, 74, 023527
Adelman-McCarthy, J. K., et al. 2007, ApJS, 172, 634
Bailin, J., et al. 2005, ApJ, 627, L17
Barkana, R., & Loeb, A. 1999, ApJ, 523, 54
Belokurov, V., et al. 2006, ApJ, 642, L137
———. 2007, ApJ, 654, 897
———. 2008, ApJ, 686, L83
Benson, A. J., Frenk, C. S., Lacey, C. G., Baugh, C. M., & Cole, S. 2002, MNRAS, 333, 177
Bertschinger, E. 2006, Phys. Rev. D, 74, 063509
Bothun, G. D., & Thompson, I. B. 1988, AJ, 96, 877
Bullock, J. S., Kravtsov, A. V., & Weinberg, D. H. 2000, ApJ, 539, 517
Cembranos, J. A., Feng, J. L., Rajaraman, A., & Takayama, F. 2005, Phys. Rev. Lett., 95, 181301
Chen, J., Kravtsov, A. V., Prada, F., Sheldon, E. S., Klypin, A. A., Blanton, M. R., Brinkmann, J., & Thakar, A. R. 2006, ApJ, 647, 86
de Jong, J. T. A., et al. 2008, ApJ, 680, 1112
Diemand, J., Kuhlen, M., & Madau, P. 2007a, ApJ, 657, 262
———. 2007b, ApJ, 667, 859
Diemand, J., Kuhlen, M., Madau, P., Zemp, M., Moore, B., Potter, D., & Stadel, J. 2008, Nature, 454, 735
Diemand, J., Moore, B., & Stadel, J. 2004, MNRAS, 352, 535
Dutton, A. A., van den Bosch, F. C., Dekel, A., & Courteau, S. 2007, ApJ, 654, 27
Faltenbacher, A., Jing, Y. P., Li, C., Mao, S., Mo, H. J., Pasquali, A., & van den Bosch, F. C. 2008, ApJ, 675, 146
Frieman, J., et al. 2005, preprint (astro-ph/0510346)
Grebel, E. K., Gallagher, J. S., III, & Harbeck, D. 2003, AJ, 125, 1926
Grillmair, C. J. 2006, ApJ, 645, L37
Hofmann, S., Schwarz, D. J., & Stoecker, H. 2001, Phys. Rev. D, 64, 083507
Hogan, C. J., & Dalcanton, J. J. 2000, Phys. Rev. D, 62, 063511
Irwin, M. J., Ferguson, A. M. N., Huxor, A. P., Tanvir, N. R., Ibata, R. A., & Lewis, G. F. 2008, ApJ, 676, L17
Irwin, M. J., et al. 2007, ApJ, 656, L13
Ivezic, Z., et al. 2008, preprint (arXiv: 0805.2366)
Johnson, M. C., & Kamionkowski, M. 2008, preprint (arXiv: 0805.1748)
Kaiser, N., et al. 2002, SPIE, 4836, 154
Kaplinghat, M. 2005, Phys. Rev. D, 72, 063510
Kaufmann, T., Wheeler, C., & Bullock, J. S. 2007, MNRAS, 382, 1187
Keller, S. C., et al. 2007, Publ. Astron. Soc. Australia, 24, 1
Klypin, A., Kravtsov, A. V., Valenzuela, O., & Prada, F. 1999, ApJ, 522, 82
Klypin, A., Zhao, H., & Somerville, R. S. 2002, ApJ, 573, 597
Koposov, S., et al. 2008, ApJ, 686, 279
Kravtsov, A. V., Gnedin, O. Y., & Klypin, A. A. 2004, ApJ, 609, 482
Kroupa, P., Theis, C., & Boily, C. M. 2005, A&A, 431, 517
Kuhlen, M., Diemand, J., & Madau, P. 2007, ApJ, 671, 1135
Madau, P., Diemand, J., & Kuhlen, M. 2008, ApJ, 679, 1260
Majewski, S. R., et al. 2007, ApJ, 670, L9
Martin, N. F., de Jong, J. T. A., & Rix, H.-W. 2008, ApJ, 684, 1075
Martin, N. F., Ibata, R. A., Chapman, S. C., Irwin, M., & Lewis, G. F. 2007, MNRAS, 380, 281
Martin, N. F., Ibata, R. A., Irwin, M. J., Chapman, S., Lewis, G. F., Ferguson, A. M. N., Tanvir, N., & McConnachie, A. W. 2006, MNRAS, 371, 1983
Mateo, M. L. 1998, ARA&A, 36, 435
McConnachie, A., et al. 2008, ApJ, in press (arXiv: 0806.3988)
McConnachie, A. W., & Irwin, M. J. 2006, MNRAS, 365, 1263
Metz, M., Kroupa, P., & Jerjen, H. 2007, MNRAS, 374, 1125
Moore, B., Ghigna, S., Governato, F., Lake, G., Quinn, T., Stadel, J., & Tozzi, P. 1999, ApJ, 524, L19
Orban, C., Gnedin, O. Y., Weisz, D. R., Skillman, E. D., Dolphin, A. E., & Holtzman, J. A. 2008, ApJ, 686, 1030
Peñarrubia, J., McConnachie, A. W., & Navarro, J. F. 2008, ApJ, 672, 904
Profumo, S., Sigurdson, K., & Kamionkowski, M. 2006, Phys. Rev. Lett., 97, 031301
Robertson, B., & Kravtsov, A. 2008, ApJ, 680, 1083
Simon, J. D., & Geha, M. 2007, ApJ, 670, 313
Somerville, R. S. 2002, ApJ, 572, L23
Stewart, K. R., Bullock, J. S., Wechsler, R. H., Maller, A. H., & Zentner, A. R. 2008, ApJ, 683, 597
Strigari, L. E., Bullock, J. S., & Kaplinghat, M. 2007a, ApJ, 657, L1
Strigari, L. E., Bullock, J. S., Kaplinghat, M., Diemand, J., Kuhlen, M., & Madau, P. 2007b, ApJ, 669, 676
Strigari, L. E., Bullock, J. S., Kaplinghat, M., Simon, J. D., Geha, M., Willman, B., & Walker, M. G. 2008a, Nature, 454, 1096
Strigari, L. E., Kaplinghat, M., & Bullock, J. S. 2007c, Phys. Rev. D, 75, 061303
Strigari, L. E., Koushiappas, S. M., Bullock, J. S., Kaplinghat, M., Simon, J. D., Geha, M., & Willman, B. 2008b, ApJ, 678, 614
Walsh, S. M., Jerjen, H., & Willman, B. 2007, ApJ, 662, L83
Walsh, S. M., Willman, B., Sand, D., Harris, J., Seth, A., Zaritsky, D., & Jerjen, H. 2008, ApJ, 688, 245
Wang, Y., Yang, X., Mo, H. J., Li, C., van den Bosch, F. C., Fan, Z., & Chen, X. 2008, MNRAS, 385, 1511
Whiting, A. B., Hau, G. K. T., Irwin, M., & Verdugo, M. 2007, AJ, 133, 715
Willman, B., Governato, F., Dalcanton, J. J., Reed, D., & Quinn, T. 2004a, MNRAS, 353, 639
———. 2004b, MNRAS, 353, 639
Willman, B., et al. 2005, AJ, 129, 2692
Yee, H. K. C., Gladders, M. D., Gilbank, D. G., Majumdar, S., Hoekstra, H., & Ellingson, E. 2007, in ASP Conf. Ser. 379, Cosmic Frontiers, ed. N. Metcalfe & T. Shanks (San Francisco: ASP), 103
Zentner, A. R., & Bullock, J. S. 2003, ApJ, 598, 49
Zentner, A. R., Kravtsov, A. V., Gnedin, O. Y., & Klypin, A. A. 2005, ApJ, 629, 219
Zucker, D. B., et al. 2006a, ApJ, 650, L41
———. 2006b, ApJ, 643, L103